



CHORUS

This is the accepted manuscript made available via CHORUS. The article has been published as:

Entropic Description of Gas Hydrate Ice-Liquid Equilibrium via Enhanced Sampling of Coexisting Phases

Edyta Małolepsza, Jaegil Kim, and Tom Keyes

Phys. Rev. Lett. **114**, 170601 — Published 28 April 2015

DOI: [10.1103/PhysRevLett.114.170601](https://doi.org/10.1103/PhysRevLett.114.170601)

Entropic Description of Gas Hydrate Ice/Liquid Equilibrium via Enhanced Sampling of Coexisting Phases

Edyta Małolepsza and Tom Keyes*

Department of Chemistry, Boston University, Boston, MA 02215-2521

Jaegil Kim

Broad Institute of MIT and Harvard, Cambridge, MA 02142, USA

Metastable β ice holds small guest molecules in stable gas hydrates, so its solid/liquid equilibrium is of interest. However, aqueous crystal/liquid transitions are very difficult to simulate. A new MD algorithm generates trajectories in a generalized NPT ensemble and equilibrates states of coexisting phases with a selectable enthalpy. With replicas spanning the range between β ice and liquid water we find the statistical temperature from the enthalpy histograms and characterize the transition by the entropy, introducing a general computational procedure for first-order transitions.

PACS numbers: 05.10.-a, 02.70.Rr, 87.18.Bb

Gas hydrates are solutions of small guest solutes trapped in the cages of a water lattice, β ice. Many gases form hydrates under proper conditions of temperature and pressure, at concentrations 2–3 orders of magnitude greater than normal solvation for hydrophobic solutes. Methane hydrate is among the most important. Its significance for the energy sector is well appreciated, with estimates of methane held ranging from tens to hundreds times conventional reserves [1, 2]. The threat to climate of the release of methane greenhouse gas is of growing concern [3–6].

The phase equilibrium of β ice is central to hydrate formation and stability. The Gibbs free energy penalty for liquid \rightarrow β ice is small at 273 K [7], and the pressure can be increased until occupation of the cages by guests results in a thermodynamically favored hydrate.

Simulation studies are difficult because first-order phase transitions proceed through a sequence of states with coexisting phases, which are not easily sampled by conventional methods.

The root of the problem is that the entropy, $S(H)$, as a function of the enthalpy, H , exhibits a “convex intruder” interval of positive second derivative, and the statistical temperature, $T_S(H) = 1/(dS/dH)$, exhibits an S -loop (Fig. 1). Recalling van der Waals theory, the states in the coexisting enthalpy range are often called metastable and, between the extrema, unstable. However, in constant temperature simulations they are simply states with a low sampling weight. The loop arises from finite-system-size surface effects at the interfaces of the coexisting phases, not instability, as has been emphasized earlier [8–10].

The higher the barrier to the transition, the more pronounced the loop and the more difficult the simulation. In particular, the barrier for the freezing of water is very pronounced. For a constant temperature ensemble near the transition temperature (green solid line in Fig. 1), the equation, $T = T_S(H^*)$, for the extrema, H^* , of the enthalpy distribution has three solutions, two maxima and a minimum, corresponding to the low and high enthalpy states, H_1 and H_2 , of the transition and the barrier, H_{bar} . These points correspond to two minima and a maximum in the Gibbs free energy profile at the indicated temperature. The coexisting states around the barrier are rarely visited and the system is stuck in one of the free energy minima.

With a high barrier, strong supercooling or superheating, and nonequilibrium processes, are required to drive the transition, possibly distorting the results. That is, T is not a good control variable [10–13], a primary cause of the challenge of understanding the mechanism of hydrate formation [14–19]. Therefore, alternatives to isothermal-isobaric algorithms, which have been used almost exclusively for hydrate simulations, are desirable.

In the following we use the generalized replica exchange method (gREM) [20] with an optimally-designed sampling weight, $W_\alpha = \exp(-w_\alpha(H))$, w_α being the effective potential in replica α . For a comprehensive sampling of phase-coexistence states, which are inaccessible in a constant-temperature ensemble, we tailored the effective potential, $w_\alpha(H) = \int^H (1/T_\alpha(H'))dH'$, with an enthalpy-dependent generalized temperature,

$$T_\alpha(H) = \lambda_\alpha + \eta(H - H_0), \quad (1)$$

H_0 being the reference enthalpy. Using a sufficiently large negative η ensures a single intersection between $T_\alpha(H)$ and $T_S(H)$, and the resulting enthalpy distributions become unimodal at H_α^* , determined by $T_\alpha(H_\alpha^*) = T_S(H_\alpha^*)$. Since, for a given slope η , the value of H_α^* is controlled by the parameter λ_α , varying λ_α allows exploration of the phase-coexistence using enthalpy as the control variable, with two phases smoothly joined via a succession of unimodal distributions.

Previously the gREM has been implemented as a generalized Monte Carlo algorithm [20–23]. Here we introduce a faster constant pressure molecular dynamics (MD) version, by treating the volume as an additional coordinate [24]

and introducing effective potential $k_B T_0 w_\alpha(H)$, where $H = U + p_0 V$, p_0 is the pressure, and T_0 is the ‘kinetic’ temperature. Then, isothermal-isobaric MD at T_0 samples the desired weight. The forces are those of the true potential, U , scaled by $(T_0/T_\alpha(H))$. Separating T_0 , which controls the velocities, from the configurational $T_\alpha(H)$ allows sampling of low-enthalpy configurations with fast particles. The method was implemented by our group as a module in LAMMPS [25, 26].

MD gREM simulations, the first for a bulk water crystal/liquid transition, were performed for 2944 waters in 54 replicas under pressure of 1 atm and $T_0 = 330$ K, and initially in perfect β ice configurations in symmetry SI, using the mW coarse-grained model [17] with periodic boundary conditions.

Although β ice is never the thermodynamically stable state, the barrier to stable hexagonal α ice insures that it will not be sampled under these conditions and the metastable β ice-liquid transition is well defined in the restricted configuration space.

Representative mixed-phase configurations across the transition from β ice to liquid water, stabilized in equilibrium by gREM, are displayed in Fig. 2. The observed states are β ice, ice with a small spherical liquid region, a cylinder of liquid in ice, two types of slabs of ice and liquid with a flat interface differing by the number of layers of β ice cages, and finally liquid.

Videos of simulations starting from β ice and leading to coexisting states of β ice and liquid water in stable equilibrium can be found in the Supplementary Materials. For these simulations we used generalized quenching, switching $T_\alpha(H)$ so it crosses $T_S(H)$ at the desired final enthalpy in single replica simulations.

Mixed-phase configurations in Fig. 2 are separated by barriers. Fig. 3 shows the enthalpy versus time for the replicas around these barriers, top, and the enthalpy histograms for all the replicas, bottom. Exchanges involving configurations on different sides of a barrier, especially for liquid water and a slab of liquid and ice (top two replicas in Fig. 3) are infrequent due to the barrier, which is not surprising given the difficulty of simulating the freezing of water. Nevertheless, in contrast to what would be found with constant- T simulations, they do occur. The coexistence regime is well covered.

We applied the ST-WHAM method [13], a non-iterative alternative to the original WHAM [27], to efficiently combine data from multiple replicas by determining a piece of T_S in each replica from the enthalpy histogram, and merging them to form the complete T_S function.

The statistical temperature is shown in Fig. 4(a), along with its inverse, $\beta_S(H)$, in Fig. 4(b). An S -loop with considerable structure is apparent. The maximum and minimum of $T_S(H)$ are the limits of stability of the homogeneous phases, 341.4 K and 207.8 K. The upper temperature, T_u , agrees with the range 340-350 K found in the previous, isothermal-isobaric study [19], and the lower, T_l , is above that given for the mW α ice-liquid transformation, 202 K [28], and so β ice does not form α ice upon melting.

The constant- T Maxwell construction becomes an equal-area construction (gray dashed areas in Fig. 4(b)) for $\beta_S(H)$ in the microcanonical ensemble, yielding the equilibrium melting temperature, $T_m = 256.4$ K (blue dashed line in Fig. 4(a)).

The enthalpy range with $\beta'_S(H) = d^2 S(H)/dH^2 > 0$ corresponds to the convex intruder (see Fig. 4(c)). In the microcanonical approach [10–12], a peak of $\beta'_S(H)$ identifies a transition, and a positive value indicates that it is first-order. The ‘‘subphase’’ transitions connect the distinct coexisting-phase states [8] shown in Fig. 2. Being governed by surface effects, they are size- and shape-dependent, and the subphase transitions should vanish in the thermodynamic limit. The transition from homogeneous β ice to ice with a liquid droplet is a version of the evaporation-condensation transition [8, 9].

The calculated transition temperature is related to a plateau in $T_S(H)$ corresponding to a system with 1/3 liquid and 2/3 ice. Melting one layer of β ice leads to a system with 1/2 liquid and 1/2 ice and to the appearance of the next plateau at ≈ 246.5 K, close to the previously published transition temperature value of 245 K [19]. Upon melting an additional layer we observe the transition with the strongest peak in $\beta'(H)$ that leads to fully liquid system. Perhaps the method of direct constant- T phase coexistence used in Ref. [19], with system volume equally divided between two phases, is related to T_S on the plateau with 1/2 liquid and 1/2 ice.

Fig. 4(d) shows the entropy to within an additive constant, $S(H) = \int^H dH'/T_S(H')$, and the linear Gibbs hull, $S^G(H) = S(H_1) + (H - H_1)/T_m$, which is tangent to $S(H)$ at H_1 and H_2 . The difference, $\Delta S = S^G(H) - S(H)$, enhanced through the transition regime, is shown as $S - 4\Delta S$ (the ‘‘4’’ is arbitrarily chosen for visibility of the intruder). The maximum value of ΔS , occurring at H_{bar} and equal to 0.00105 kJ/molK, is defined as the surface entropy, ΔS_{surf} , a direct measure of the strength of surface effects [10–12], which cause the intruder and the S -loop. The hull represents the entropy of a hypotheticalal mixture of phases with no surface effects. The true entropy is lower because coexisting states are shifted to higher enthalpy by surface effects, depleting the density of states.

We write $S(H) = S(H_1) + (S(H) - S(H_1))$, use the definitions of S^G and ΔS_{surf} , and find that $\Delta S_{\text{surf}} = \Delta G_{\text{bar}}/T_m$, where ΔG_{bar} is the Gibbs free energy barrier height, demonstrating again a microcanonical route to a quantity routinely computed in the canonical ensemble. If we attribute the barrier to surface effects, ΔS_{surf} becomes an

estimator of the surface tension, $\gamma = T_m \Delta S_{\text{surf}} / \sigma$, where σ is the surface area. Evaluating σ is nontrivial. However, if the barrier occurs with the coexisting states in a slab configuration, $2L^2$ is a good approximation to σ , where L is the box length, and 2 comes from the presence of two surfaces with periodic boundary conditions [8]. In this way the β ice/liquid surface tension is determined as 26.3 mJ/m², which is close to published values for hydrate/liquid and α ice/liquid [29].

Fig. 4(d) yields the latent heat and the entropy of fusion, 4.505 kJ/mol and 17.46 J/mol K, respectively, previously estimated as 4.39 kJ/mol and 17.9 J/mol K [19].

The Gibbs free energy profile at T_m , $G(H) = H - T_m S(H)$, connecting the phases at enthalpies H_1 and H_2 , is shown in Fig. 4(e). The barrier height is estimated as 0.27 kJ/mol. If we take T as the control variable, the Gibbs free energy, now evaluated as $H(T_S) - T_S S(T_S)$, is triple-valued in the coexistence regime, with equilibrium corresponding to the lowest branch and the transition at the crossing of the two lower branches (Fig. 5). Clearly, using enthalpy as the control variable gives a simpler description.

Our results suggest a unified computational entropic approach to the study of first-order transitions that is capable of treating even the crystal/liquid case in water:

- Simulate the system with the MD version of gREM.
- Extract the statistical temperature from the enthalpy (or energy) histogram in each replica and join them with ST-WHAM to obtain T_S .
- Analyze phase equilibrium using $\beta_S(H) = 1/T_S(H)$, identifying transition enthalpies via the peaks in β'_S .

The MD version of gREM can be used to cover an interesting range of temperature and enthalpy, or as a single simulation in a generalized quench to observe the evolution of the system to eventual stable equilibrium in a coexisting state at a selected point on the $T_S(H)$ curve. Here $T_\alpha(H)$ is decreased for all H by changing λ_α in $T_\alpha(H)$, just as the control variable, T , is decreased in an ordinary quench.

The research was supported by the U.S. Department of Energy, Office of Basic Energy Sciences, Division of Chemical Sciences, Geosciences and Biosciences under Award DE-SC0008810. We thank Profs. Bill Klein and Harvey Gould for discussions and Dr. Marek Orzechowski for help with graphics.

* Electronic address: keyes@bu.edu

- [1] E. D. Sloan and C. Koh, *Ed. Clathrate Hydrates of Natural Gases* (CRC Press/Taylor-Francis, Boca Raton, FL, 2007).
- [2] C. Koh, A. Sum, and E. D. Sloan, *J. Appl. Phys.* **106**, 061101 (2009).
- [3] J. Kennett, K. Cannariato, I. Hendy, and R. Behl, *Spec. Publ. Ser. American Geophysical Union* **54** (2003).
- [4] A. Winguth, C. Shellito, C. Shields, and C. Winguth, *J. Clim.* **23**, 2562 (2010).
- [5] B. Phrampus and M. Hornbach, *Nature* **490**, 527 (2012).
- [6] N. Shakhova and *et al.*, *Nature Geoscience* **7**, 64 (2014).
- [7] J. H. van der Waals and J. C. Platteeuw, *Adv. Chem. Phys.* **2**, 1 (1959).
- [8] K. Binder, B. Block, and P. Virnau, *Am. J. Phys.* **80**, 1099 (2012).
- [9] L. G. MacDowell, P. Virnau, M. M. Iler, and K. Binder, *J. Chem. Phys.* **120**, 5293 (2004).
- [10] M. Bachmann, *Thermodynamics and Statistical Mechanics of Macromolecular Systems* (Cambridge University Press, Cambridge, UK, 2014).
- [11] S. Schnabel, D. Seaton, D. Landau, and M. Bachmann, *Phys. Rev. E* **84**, 011127 (2011).
- [12] D. H. E. Gross and J. Kenney, *J. Chem. Phys.* **122**, 224111 (2005).
- [13] J. Kim, T. Keyes, and J. E. Straub, *J. Chem. Phys.* **135**, 161103 (2011).
- [14] E. D. Sloan and F. Fleyful, *AIChE J.* **37**, 1281 (1991).
- [15] R. Radhakrishnan and B. L. Trout, *J. Chem. Phys.* **117**, 1786 (2002).
- [16] L. C. Jacobson, W. Hujo, and V. Molinero, *J. Am. Chem. Soc.* **132**, 11806 (2010).
- [17] L. C. Jacobson, W. Hujo, and V. Molinero, *J. Phys. Chem. B* **114**, 13796 (2010).
- [18] L. C. Jacobson, M. Matsumoto, and V. Molinero, *J. Chem. Phys.* **135**, 074501 (2011).
- [19] L. C. Jacobson, W. Hujo, and V. Molinero, *J. Phys. Chem. B* **113**, 10298 (2009).
- [20] J. Kim, T. Keyes, and J. E. Straub, *J. Chem. Phys.* **132**, 224107 (2010).
- [21] Y. Terada, T. Keyes, J. Kim, and M. Tokuyama, *AIP Conf. Proc.* **1518**, 776 (2013).
- [22] Q. Lu, J. Kim, and J. E. Straub, *J. Chem. Phys.* **138**, 104119 (2013).
- [23] Q. Lu, J. Kim, and J. E. Straub, *J. Phys. Chem. B* **116**, 8654 (2012).
- [24] H. C. Andersen, *J. Chem. Phys.* **72**, 2384 (1980).
- [25] S. Plimpton, *J. Comp. Phys.* **117**, 1 (1995).
- [26] <http://lammps.sandia.gov>.
- [27] A. M. Ferrenberg and R. H. Swendsen, *Phys. Rev. Lett.* **63**, 1195 (1989).
- [28] E. B. Moore and V. Molinero, *Nature* **479**, 506 (2011).
- [29] R. Anderson, M. Llamedo, B. Tohidi, and R. W. Burgass, *J. Phys. Chem. B* **107**, 3507 (2003).

Figures

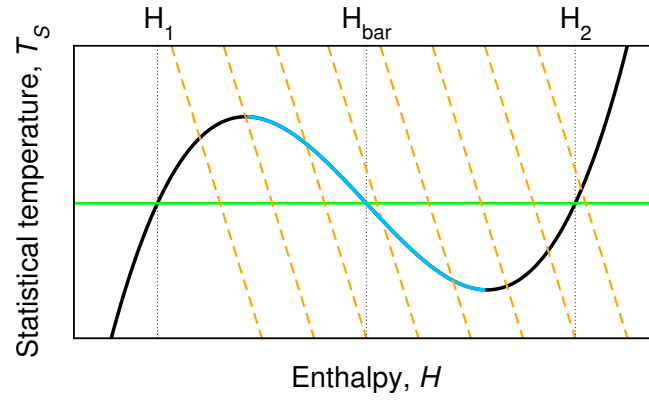


FIG. 1: (Color online) With an S -loop the statistical temperature (black, blue) intersects the green constant- T line at H_1 , H_{bar} , and H_2 . Blue line represents region of coexisting states with strong surface effects in a simulation, or unstable states in a van der Waals model. Orange dashed lines are examples of generalized temperature $T_\alpha(H)$, see Eq. (1).

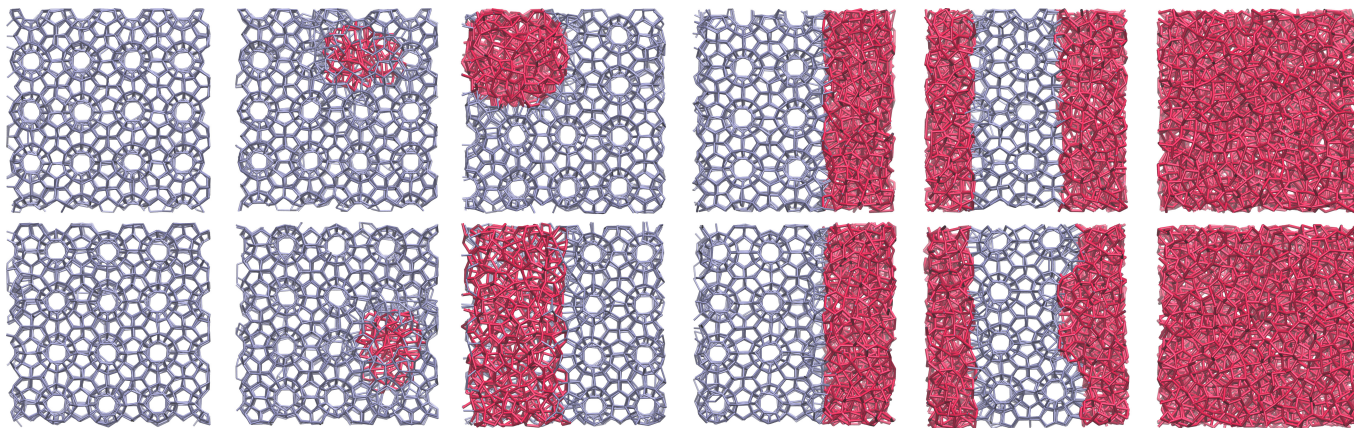


FIG. 2: (Color online) Configurations in stable equilibrium as enthalpy increases from left to right across the coexistence range: β ice, liquid droplet in β ice, liquid cylinder in β ice, slabs of liquid and ice, and liquid. Top and bottom represent top and side views with blue bonds between molecules forming β ice and red for liquid.

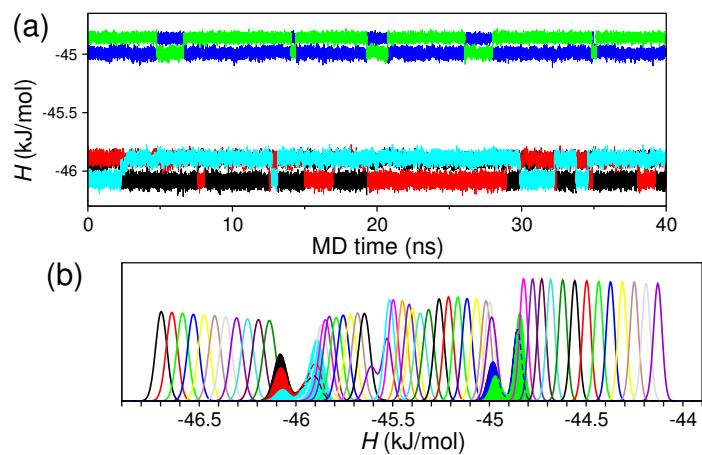


FIG. 3: (Color online) Top: Enthalpy versus time for replicas near the barriers to configurational transitions demonstrates that gREM allows exchanges for good sampling even across barriers. Bottom: Enthalpy histograms of all the replicas (replicas around barriers, shown on plot above, are in solid) show that the coexistence range is sampled without gaps.

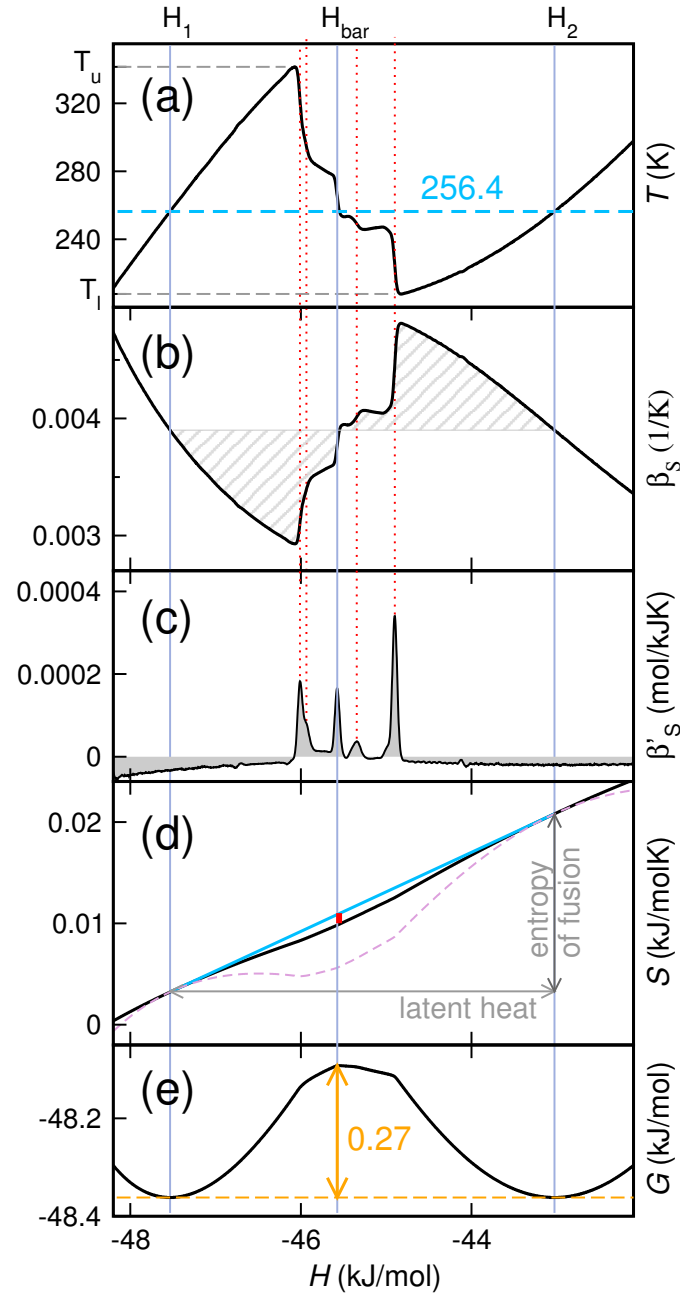


FIG. 4: (Color online) Different aspects of the β ice-liquid transition revealed by the entropic analysis: (a) the statistical temperature, $T_S(H)$, with transition temperature shown in blue. Upper and lower limits of stability shown as T_u and T_l ; (b) its inverse, $\beta_S(H)$, where equal areas used in Maxwell construction are shaded; (c) $\beta'_S(H)$ with peaks identifying subphase transitions; (d) entropy $S(H)$ in black, Gibbs hull in blue connects inflection points on entropy curve, entropy with magnified deviation from Gibbs hull as $S - 4\Delta S$ in violet (to enhance visibility of convex intruder), surface entropy in red. Arrows show the latent heat and entropy of fusion; (e) Gibbs free energy profile at equilibrium transition temperature with barrier height indicated by an arrow.

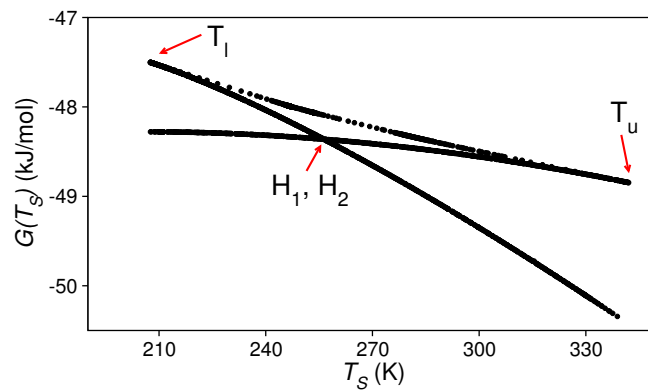


FIG. 5: (Color online) Temperature-dependent Gibbs free energy evaluated as $G(T_S) = H(T_S) - T_S S(T_S)$ with closed loop characteristic of first-order phase transition. The crossing point corresponds to points H_1 and H_2 in Fig. 4, where the coexisting phases have equal free energy, while the turning points correspond to T_l and T_u , the limits of stability.